Effect of Glabridin on the Structure of Ileum and Pancreas in Diabetic Rats: A histological, Immunohistochemical and Ultrastructural Study

Maha M. Abo Gazia[1] and Nermeen M. Hasan[2]

[1]Histology Department, Faculty of Medicine, Al-Fayoum University
[2]Medical Biochemistry Department, Faculty of Medicine, Cairo University
mahaabogazia@yahoo.com

Abstract: The ileum and pancreas exhibit numerous morphological and functional changes in streptozotocin (STZ)-induced diabetes. Glabridin, a major flavonoid of Glycyrrhiza glabra (licorice), possesses multiple pharmacological activities. This study was carried out to clarify the role of glabridin on immunohistochemical and ultrastructural changes and associated oxidative stress in ileum and pancreas of diabetic rats. For this purpose, 30 adult male albino rats were divided into 3 groups (10 animals each); control group, diabetic group and the third group was concomitantly subjected to both induction of diabetes and glabridin treatment. After 28 days all animals were sacrificed and specimens from ileum and pancreatic cells were processed for light and electron microscopic examinations, morphometric analysis with immunohisto-chemical staining of pancreatic beta-cells by anti-insulin antibody. H and E stained ileal sections in diabetic rats exhibited, pleomorphism of villi, with erosion of their apical columnar epithelial cells and cellular infiltrations. Homogeneous material with increased crypt depth, goblet cell numbers and thickness of muscularis layer were also observed, using Scanning electron microscope, ileal villi appeared wider with marked convolutions and minimal loss of microvilli. Pancreatic β-cells ultrathin sections in the diabetic group showed shrinkage nuclei, depletion of β-cells granules, vacuolation and dissolution of mitochondria. Insulin immunoreactivity was apparently reduced by about 50% from total β-cell bulk in diabetic group. Glabridin treatment significantly reduced the observed histological alterations and morphometric changes in the ileum and pancreatic islet cells in diabetic rats. Biochemically, there was a significant increase in lipid peroxidation and oxidative stress markers, namely superoxide dismutase (SOD), catalase with decline in glutathione peroxidase, increased levels of blood glucose, glycohaemoglabin, cholesterol and low density lipoprotein (LDL) in group II. These parameters returned to normal respective values after glabridin treatment. Conclusion: Glabridin administration ameliorates diabetes-induced ileal mucosa and pancreatic β-cells morphological and biochemical changes with their associated oxidative stress.

[Maha M. Abo Gazia and Nermeen M. Hasan Effect of Glabridin on the Structure of Ileum and Pancreas in Diabetic Rats: A histological, Immunohistochemical and Ultrastructural Study. Nature and Science 2012; 10(3):78-90]. (ISSN: 1545-0740). http://www.sciencepub.net 12

Key Words: Glabridin, Ileum, Pancreas, Diabetic rats, anti-insulin antibody.

1. Introduction

Diabetes mellitus is a chronic disease characterized by hyperglycemia, with alterations in cellular metabolism ***(Zoubi et al., 1995)***. Hyperglycemia is responsible for causing metabolic disturbances, such as oxidative stress, which lead to injuries in different cellular types of gastrointestinal tract and impair endogenous antioxidant defense system ***(Bhor et al., 2004)***. Oxidative stress is believed to play a role in development of small intestine complications. The intestinal mucosa is vulnerable to oxidative stress on account of constant exposure to reactive oxygen species (ROS) generated by the luminal contents such as oxidized food debris and bacterial metabolites ***(Ettarh and Carr, 1997)***.

Various experimental studies suggested that oxidative stress impaired pancreatic β-cell insulin secretion via pancreatic β-cell lysis through DNA fragmentation ***(Evan et al., 2003)***. Also, free radicals have been shown to disrupt insulin action and total b

Liquorice (Glycyrrhize glabra) is a widely used medicinal plant, and has been used for ages in herbal therapy for curing inflammatory responses, bacterial and viral diseases ***(Sen et al., 2011)***. Glabridin, phytoestrogen from licorice root, has been found to exhibit potent antioxidative activity, superoxide-scavenging activities in biological membranes, inhibit mitochondrial lipid peroxidation, protected respiratory-enzyme activities in the mitochondrial electron transport system against oxidative stresses ***(Nakagawa et al., 2004)*** and in prevention of low-density lipoprotein oxidation ***(Fukai et al., 2003)***. The aim of the present work is to study the effects of glabridin on histological, immunohistochemical and ultrastructural changes and associated oxidative stress in of streptozotocin STZ-induced diabetic rats.

2. Material and Methods

The present study was conducted on 30 adult

male albino rats weighing 230 – 280g at the beging of experiment, with free access to water *ad-libitum*. The animals were acclimatized for 7 days before experiment and divided into three main groups.

- **Group I (control group):** formed of 10 rats. This group was further subdivided into two equal groups.
- **Subgroup Ia :** formed of 5 rats that received balanced standard diet according to ***Rumpler et al. (1998)***.
- **Subgroup Ib:** formed of 5 rats that received balanced diet together with glabridin. Glabridin was given by oral rout to mice at dose of 30 mg/kg b.wt. daily for 14 days according to ***Fukai et al. (2003)*** and prepared as water soluble and given by stomach tube.
- **Group II (Diabetic group):** formed of 10 rats that received single intraperitoneal injection of streptozotocin in a dose level 60mg/kg b.wt.
- **Group III (Glabridin treated diabetic rat):** formed of 10 diabetic rats treated with glabridin for two weeks after diabetes induction.

Induction of Diabetes Mellitus:

Diabetes was induced by single intraperitoneal injection of streptozotocin (Sigma Chemical Company), St. Louis, MO, USA in a dose of 60mg/kg body weight dissolved in 0.01M citrate buffer, pH 4.5 according to ***Sen et al. (2011)***. After 48 hours, blood samples were obtained from their orbital sinuses for assay of blood glucose level. Induction of diabetes was monitored for 28 days by whole blood glucose estimation. Only animals with blood glucose levels >200mg/dL were considered as diabetic according to ***Sen et al. (2011)***. At the appropriate time, rats were sacrificed at the 28th day of the experiment after injection of thiopental sodium (Abbott Labs, USA) at a dose of 40 mg/kg b. wt, I.P injection of thiopental sodium (Abbott Labs, USA) at a dose of 40 mg/kg b. wt, I.P. Venous blood was obtained from the animals of all groups, centrifuged and the sera were stored at -70^{o}C for biochemical evaluation. Blood was sampled for hyperglycemia, hyperlipidemia and oxidative enzymes parameters.

Tissue Sampling:

For histological studies, ileal specimens were obtained from the ileum 5 cm proximal to the ileo-cecal valve. Within a short time, the residual contents in the lumen were cleared using saline. Specimens were fixed in 10% formalin for one day, processed and embedded in paraffin blocks. The slides were stained with hematoxylin-Eosin and studied by light microscope. For scanning electron microscopic examination, the specimens were immediately fixed in 1.5% glutraldehyde solution in phosphate buffer solution. Then, they were post-fixed in 1% phosphate buffer in osmium tetra-oxide, dehydrated in acetone and dried in critical point drier apparatus. There after, the dried samples were mounted on stubs, coated with a thin layer of gold and the ileal mucosa were examined by routine protocol by (JSM-5300) scanning electron microscope (JEOL, Tokyo, Japan) in the Faculty of Medicine, Tanta University ***(Hayat, 1981)***.

Pancreatic pieces from control and other groups were fixed in Bouin's fluid for routine H and E stain. The other pieces were fixed in 3% phosphate buffer glutaraldehyde for 3hrs at – 4, post-fixed in buffered osmium tetroxide, dehydrated in ethanol and embedded in araldite. The ultrathin sections were placed in copper grids, doubly stained with urinayl acetate followed by lead citrate to be examined by (JEM-1010) transmission electron microscope (TEM; JEOL, Tokyo, Japan) in Tanta University, Faculty of Medicine.

For immunohistochemical study, immunohistochemical staining was performed on formaline-fixed, paraffin-embedded pancreas from all groups and primary antibodies for rat insulin were supplied by Bio Genex Cat. No. AR. 295-R. Then, the sections were counterstained with Mayer's haematoxylin ***(Kiernan, 2000)***.

Morphometeric Analysis:

Briefly as described by ***Ettarh et al., (1997)*** circumferential values of villi height, crypt depth and muscularis layer thickness were measured using an automatic analysis system ***(Kow, 1977)***. Only villous profiles with stromal core that showed continuity at their basis with the inter-cryptal stroma (attached villi) were counted. Also, only crypt profiles which abutted the inner-muscle layer were counted, while those not in contact with muscle layer were excluded since they were assumed to represent sections through the upper parts of inclined crypts. Only crypt profiles with 9 or more cells were counted. As regard pancreas morphometry, briefly as reported by ***Adeyemi et al., (2010)*** islet profiles were examined at different magnifications in the non-serial pancreatic sections to estimate (a) number of islets in each section of pancreas (b) the diameter of the islets (c) the number of β-cells of the pancreatic islets. The β-cells were determined by direct counting method at 1000 x magnification. The number of islets were quantified at these sections at 40 x magnification. The data were obtained using Leica Quin 500 MC image analyzer computer system in Faculty of Medicine, Cairo University.

Biochemical Study:

Markers of oxidative stress:

(A) Lipid peroxidation:

Tissue malondialdehyde (MDA) (Digilab Hitachi U-2800, Tokyo, Japan) level, the end product of fatty acid peroxidation was used as indicator of lipid peroxidation, measured spectrophotometrically by measuring of the color produced during the reaction with thiobarbituric acid (TBA) with MDA at 532nm. The results were expressed as nmol of MDA/mg protein ***(Esterbauer and Cheeseman, 1990)***.

(B) Antioxidant status:

1. Tissue glutathione peroxidase (Cat. No.: CGP1, Sigma-USA) activity was assayed by colorimetric method. The reduced glutathione was measured at 412nm by spectrophotometer. Enzyme activity was expressed as µg of glutathione oxidized/min/mg protein according to method of ***Rotruck et al. (1973)***.
2. Tissue superoxide dismutase (Cayman Chemical Company, Catalog No.: 7006002, Ann Arbor, USA) activity was measured and expressed as U/mg protein according to the method of ***Marklund and Marklund (1974)***.
3. Catalase (Cat. No.: 100, Sigma-USA) activity was measured according to the method of ***Aebi (1993)***. The enzyme activity was expressed as K/sec/mg protein.

Determination of glycemic status:

(a) Plasma glucose levels were estimated by the glucose oxides peroxidase method ***(Tinder, 1969)*** and were expressed as mg/dL. Glycosylated hemoglobin was measured and expressed in terms of % ***(Chandalia et al., 1980)***.

(b) Determination of lipid profiles (cholesterol level and triglyceides) was measured by enzymatic methods ***(Wybenga et al., 1970; McGowan et al., 1983)***.

- **Blood Glucose, Glycosylated Hb%, Cholesterol, Triglyceides Prchased from (Sigma. Aldrich, St. Louis, USA).**

Statistical Analysis:

The data were representative of normal distribution and the results were expressed as means ± SD. Comparisons between all groups were analysed using student t-test ***(Goldstone, 1983)***. A probability value of $P < 0.05$ was considered to indicate statistical significances, and highly significant with $P < 0.001$ while values of $P > 0.05$ were considered statistically nonsignificant ***(Dawson and Trapp, 2001)***.

4. RESULTS:

I- Histological results:

(A) Small intestine (Ileum):

Light microscopic results:

Group I (control group):

In H and E-stained sections, the ileal villi were seen to be covered with tall columnar cells (enterocytes) with oval basal vesicular nuclei. The villi are interposed by shallow clefts, slightly elongated with short ridge-like shape and connective tissue core are surrounded by the epithelial layer. Crypts of Leiberkuhn, the openings between the bases of these villi, are simple tubular glands, extended down to muscularis mucosa. These crypts are appeared like invginations of mucosa between the bases of the ileal villi. Goblet cells are seen to be present between the enterocytes at intervals (Fig.1). The height of the villi showed a mean value of 312 µm ± 14.2 and 314 µm ± 2.29. As regards to the other morphometric analysis data, , crypt depth and muscularis muscle layer thickness was calculated to be 195 µm ± 5.11, 194 µm ± 5.13, 95.54 µm ± 3.30 and 93.92 µm ± 3.233, respectively (Table 3).

Group II (Diabetic group):

The sections showed disturbed villous architecture, thick villi with discontinuous epithelium, cellular infiltration and edema in the core of villi (Fig. 2). Other villous assuming conical forms, loss of epithelial covering especially at the tip, ill-defined increased number of goblet cells were noticed between columnar cells (Fig. 3). In addition to villous and crypt hypertrophy, ileal villi varied in shape with many of these villi appeared twisted, some assuming laterally collapsed on the neighbouring villi, there is separation of the epithelium from the underlying corium (Figs. 4-6). The mean value of height of villi, crypt depth and muscularis muscle layer thickness was calculated to be 476 µm ± 32.1, 235 µm ± 0.40 and 12.63 µm ± 4.43, respectively. As seen in diabetic group the height of villi shows a significant increase in comparison to control animals ($P<0.001$) but without significant difference between glabridin treated diabetic rats and control rats. The crypt depth and muscle layer thickness are significantly higher than control groups ($P < 0.001$) (Table 3).

Group III (glabridin treated diabetic rat):

Diabetic animals received glabridin for 28 days, the villi showed slight hypertorphic changes, moderate lymphocytes infiltration with no apical

changes (Fig. 7). In the ileum there is no significant difference between glabridin treated diabetic and control group. The mean value of the hight of villi, crypt depth and muscularis layer thickness was calculated to be 342 µm ± 15.3, 210 µm ± 10.50 and 111.20 µm ± 6.83 respectively. There are a significant decrease in villi height, crypt depth and muscle layer thickness to near normal values after glabridin treatment (Table 3).

Scanning electron microscopic results:
Group I (Control group):

Ileal villi appeared normal with intact surface epithelium. The villous surface showed a velvet, hexagonal appearance with mucous of the goblet cells. The normal microvilli were packed together with a uniform shape (Figs. 8-10).

Group II (Diabetic group):

Most of ileal villi show irregular appearance with sloughing of epithelial covering at the tips, poorly developed goblet cells and necrotic tips (Fig. 11). The villi appeared wider with some surface have marked convolutions and rough granular appearance, other surface showed of microvilli loss (Figs. 12, 13).

Group III:

Villous tips and surface revealed normal surface epithelium with goblet cells openings and some villi still show sloughing of their tips (Fig. 14). The microvilli on the enterocytes surface appeared nearly normal with mucous secretions of the numerous goblet cells with normal structure in most of villi (Figs. 15,16).

(B) Pancreas:
Light microscopic results:
Examination of sections stained with H & E from:
Group I (Control group):

Showed closely packed pancreatic acini composed of pyramidal shaped cells with rounded pale stained nuclei surrounded by basophilic cytoplasm with eosinophilic granules in the apices of the cells (the exocrine part of the pancreas. The pale-stained islets of Langerhans (the endocrine part) were scattered throughout the exocrine component (Fig. 17).

Group II (Diabetic group):

Showed severe degenerative changes of pancreatic islets with irregular out line, decrease populated cells and homogenization of the center and apparent reduction of the size and number of islets. β-cells were less frequent with degenerative and shrunken changes. Some β-cells showed nuclei packed together with variable changes, some appear vesicular and others were pyknotic. The cytoplasm lost most of the granules, some cells with foamy or clear cytoplasm and others were ballooned with vacuolated cytoplasm. Some acini showed disturbance of the acinar pattern structure, pyknotic nuclei of some acinar cells with severely damaged vacuolated cytoplasm. Congestion of blood vessels, detached endothelial liming with wide interstitial tissue were noticed in some sections (Fig.18).

Group III:

Showed nearly normal pancreatic architecture and the β-islets had retained their morphology (Fig. 19).

Immunohistochemical study:

Control group (Group I) The Beta-cells (β-cells) were appeared in immunohistochemically stained sections to form the major cells population of the islets (Fig. 20). In diabetic group (Group II) there was marked reduction in immunohistochemical reaction to insulin in β-cells of islets of Langerhans (Fig. 21). Mean while in group (III) with glabridin treatment, there was still decrease in insulin immunoreactivity in some islets. However, most of the islets showed increased in the positive imunostaining for insulin of β-cells as in control group (Fig. 22). The results of the morphometric analysis revealed a significant reduction in the numerical density of islets (number of islet/pancreas), islet diameter, numerical density of β-cells (number of β-cells per islet), in the diabetic group of rats when compared with the control group. However, these morphometric parameters were significantly increased in the glabridin treated rats when compared with those of the untreated diabetic rats.

Transmission electron microscopic results:
Group I (Control group):

Examination of specimens obtained from the control animals showed exocrine acinar cells were occupied by numerous electron-dense secretory granules of variable sizes, numerous cisternae of RER and well developed Golgi apparatus. The endocrine β-cell with dispersed chromatin in its nucleus and mitochondria, and granules have dark centeral core surrounded by an electron lucent halo (Fig. 23).

Group II:

Specimens obtained from diabetic animals revealed endocrine β-cells of islet containing vacuolized mitocheondria lost their cristae and increase in the halo spaces areas around β-granules. Dilatation of RER with damaged and vacuolized mitochondria in the exocrine cell were also observed

(Fig. 24). Other endocrine β-cells of islets revealed the presence of many β- granules with increase electron lucent halo spaces surrounded the dense core. Vacuolized and damaged mitochondria, dilated cisternae of rough endoplasmic reticulum (RER) and some electron lucent vacuoles were also noticed. other β-cell showed nucleus with euchromatin predominatnte over the heterochromatin and decrease or even deptetion of β-granules. There was marked degenerative changes in some acinar cells as manifested by decrease of secretory granules, appearance of autophagic vacuoles and destroyed mitochondria (Figs. 25, 26).

Group III:

Specimens obtained from animals of glabridin treated diabetic animals showed exocrine acinar cell with dilatation of RER and an increased amount of zymogen granules (Fig. 27) Endocrine β-cell appearently had retained their morphology and cellular organelles, also, normal shaped appearance mitochondria RER and decreased vacuotation in many islets (Fig. 28).

II- Biochemical Results:

Blood glucose, glycosylated hemoglobin, cholesterol and triglycerides:

Diabetic rats showed a significant increase in plasma glucose (P<0.001), glycosylated hemoglobin % (P<0.001), plasma cholesterol (P<0.05), and triglyceride compared to control rats. Treatment with glabridin did not significantly change plasma glucose level and glycosylated hemoglobin but resulted in a significant decrease in plasma cholesterol and triglycerides levels (P < 0.001) (Table 1).

Changes in lipid peroxidation and oxidative enzymes:

Compared with control group, the diabetic group exhibited a significant increase in lipid peroxidation tissue antioxidant components, such as catalase, superoxide dismutase were increased while glutathione peroxidase, was significantly decreased in diabetic group (P < 0.001). Glabridin treatment in diabetic rats decreased lipid peroxidation and increased antioxidant enzyme levels nearly to normal values (Table 2).

Table (1): Effect of diabetes and glabridin on plasma glucose, glycosylated hemoglobin (%), cholesterol and triglyceride levels in control and different group

Parameters	Control group		Diabetic Group	Glabridin Treated Diabetic Group
	-ve Control	Glabridin		
Plasma glucose (mg/dL)	124.2±3.2	126.1±3.1	345.2±13.6[a]	302±13.7
Glycosylated hemoglobin (%)	3.3±0.2	3.2±0.3	6.2±0.3[a]	5.8±0.2
Cholesterol (mg/dL)	71.82±4.8	68.21±7.5	76.31±7.9[a]	68.33±3.6[b]
Triglyceride (mg/dL)	50.98±8.12	53.03±7.33	60.33±5.2[a]	49.02±6.4[b]

Values are expressed as mean ± S.D. [a] P<0.001 as compared to control. [b] P<0.001 as compared to diabetic.

Table (2): Changes in the levels of lipid peroxidation and antioxidant enzymes in control and different treated groups.

Groups	Control group		Diabetic Group	Glabridin Treated Diabetic Group
	-ve Control	Glabridin		
Lipid peroxidation (nmol MDA/mg protein)	0.172±0.06	0.170±0.05	0.715±0.07[a]	0.169±0.06[b]
Glutathione peroxidase (µg of glutathione oxidized/min/mg/protein)	2.883±0.581	2.880±0.583	0.932±0.208[a]	2.878±0.582[b]
Superoxide dismutase U/mg protein)	7.532±1.052	7.558±1.055	12.952±1.372[a]	7.533±1.055[b]
Catalase κ/sec/mg protein	0.026±0.002	0.023±0.002	0.058±0.007[a]	0.023±0.003[b]

Values are expressed as mean ± S.D.[a] P<0.001 as compared to control. [b] P<0.001 as compared to diabetic.

Table (3): Changes in villi height, crypt depth, muscle layer thickness number of β-cell, number of islet and diameter of islets.

Groups	Control group		Diabetic Group	Glabridin Treated Diabetic Group
	-ve Control	Glabridin		
Villi height (µm)	312±14.2	314±2.29	476±32.1[a]	342±15.31[b]
Grypt depth (µm)	195±5.11	194±5.13	235±8.40[a]	210±10.50[b]
Muscularis layer thickness (µm)	95.54±3.30	93.92±3.23	12.63±4.43[a]	111.20±6.83[b]
Number of β-cells/islet (N/1000µm^2)	10.66±0.729	10.71±0.722	2.88±0.361[a]	8.62±0.189[b]
Number of islets/pancreas (N/10mm^2)	18.77±0.729	18.29±0.735	5.78±0.445[a]	12.52±0.562[b]
Diameter of islets (µm)	131.78±12.819	132.70±12.811	63.76±8.415[a]	89.92±11.705[b]

Values are expressed as mean ± S.D. [a] P<0.001 as compared to control. [b] P<0.001 as compared to diabetic.

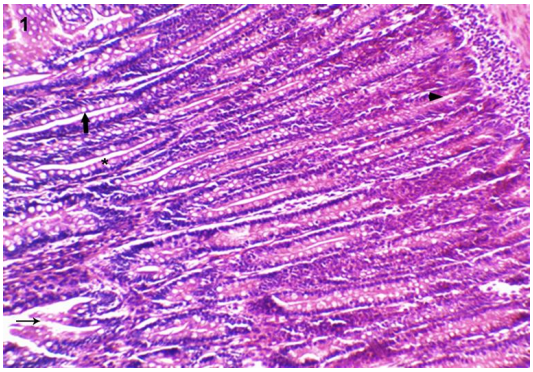

Fig. (1): A photomicrograph of a section of rat ileum from control group showing ileal mucosa with finger like projections of the villi (→) and invaginated crypts of leiberkuhn between the bases of the villi (►).tall columnar cells of enterocytes with oval basal nuclei and regular continuous brush border (*) with goblet cells inbetween the enterocytes (⟨). (H & E, Mic. Mag. 200)

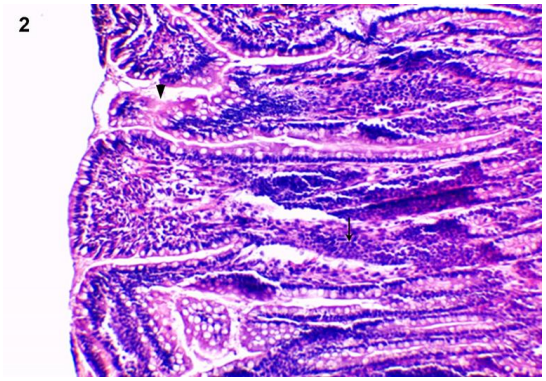

Fig. (2): A photomicrograph of a section of rat ileum from diabetic group showing disturbed villous architecture, thick villous with discontinuous epithelium (►), cellular infiltration and edema in the core of villi (→).

(H & E, Mic. Mag. x 200)

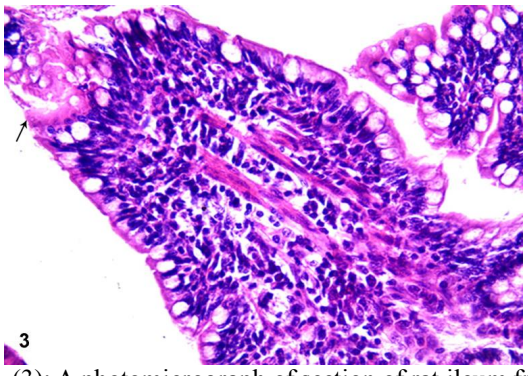

Fig. (3): A photomicrograph of section of rat ileum from diabetic group showing a villous assuming conical forms, loss of epithelial covering especially at the tip (→) with ill-defined increased number of goblet cells. (H & E, Mic. Mag. x 400)

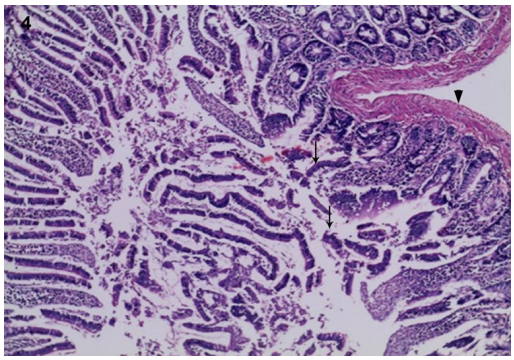

Fig. (4): Photomicrographs of section of rat ileum from diabetic group showing increase height of villi and depth of the crypts, villi appeared twisted and assuming laterally collapsed on the neighbouring villi, there is separation of the epithelium from the underlying corium (→) and thick muscle layer (►).

(H & E, Mic. Mag. x 200)

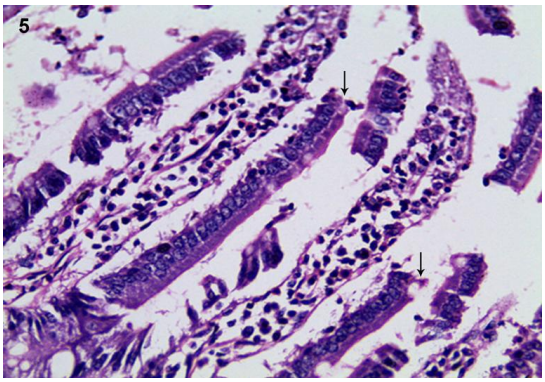

Fig. (5): A photomicrograph of a section of rat ileum from glabridin treated diabetic group showing villi with complete separation of the epithelium from the underlying corium (→). (H & E, Mic. Mag. x 400)

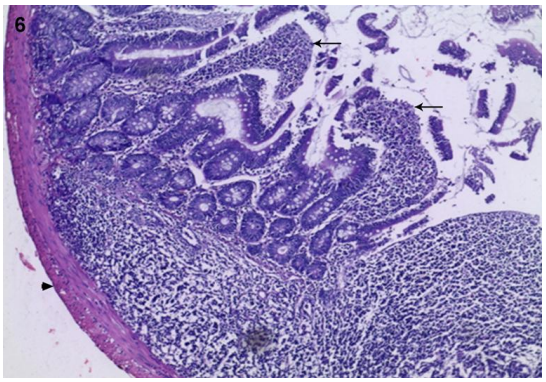

Fig. (6): A photomicrograph of a section of rat ileum from glabridin treated diabetic group showing villi with discontinous epithelium cellular infiltration (→) and increase thickness of muscle layer (►). (H & E, Mic. Mag. x 200)

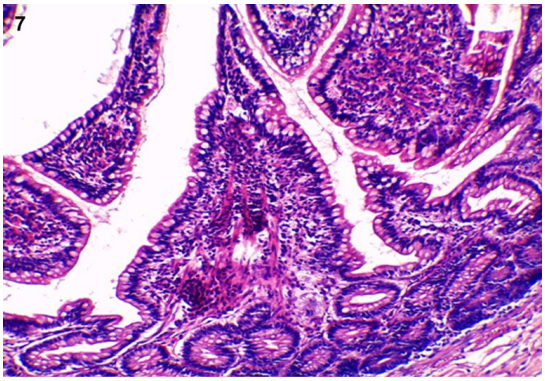

Fig. (7): A photomicrograph of a section of rat ileum from glabridin treated diabetic group showing more or less normal villi. (H & E, Mic. Mag. x 200)

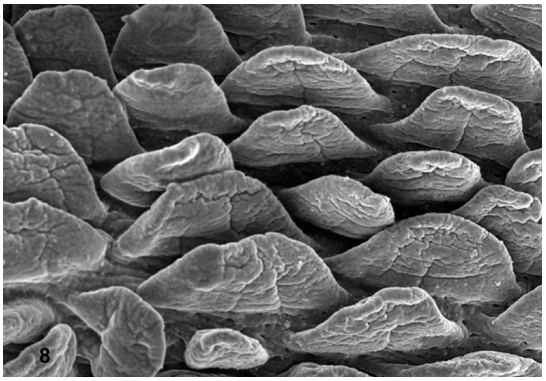

Fig. (8): Scanning electron micrograph of ileal villi of control group showing intact surface columnar epithelium with ridge shaped. (x 100)

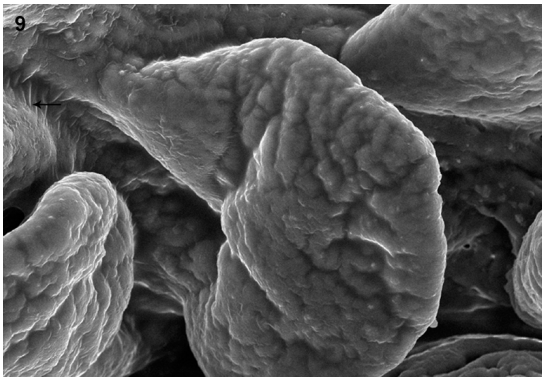

Fig. (9): Scanning electron micrograph of ileal villi of control group showing intact villous tips with velvet hexagonal appearance and generally smooth surface. The microvilli were packed together with uniform shape (→). (x 350)

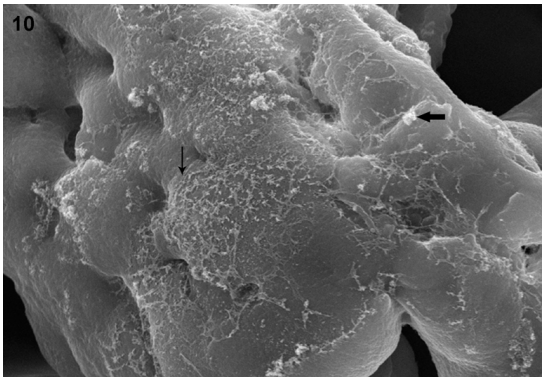

Fig. (10): Scanning electron micrograph of ileal villi of control group showing the surface is rough in appearance due to the microvilli of columnar epithelial cells (→) with mucous of goblet cells (◊). (x 2000)

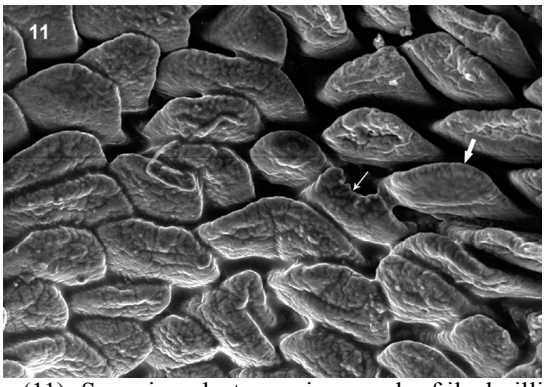

Fig. (11): Scanning electron micrograph of ileal villi of diabetic group showing most of the villi with irregular appearance and necrotic tips and sloughing of epithelial covering at the tips of some villi (→) and some villi showed normal appearance (⟨). (x 100)

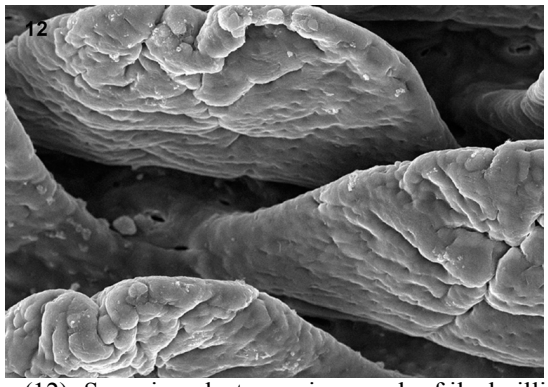

Fig. (12): Scanning electron micrograph of ileal villi of diabetic group showing villous appeared wider with some surface have marked convolutions and rough granular appearance. (x 350)

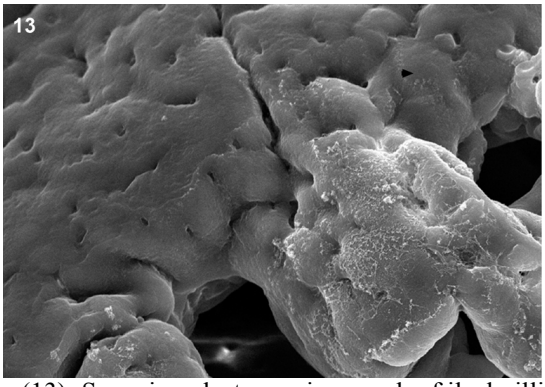

Fig. (13): Scanning electron micrograph of ileal villi of diabetic group showing a surface of villous with smooth areas due to loss of microvilli (►) (x 1000)

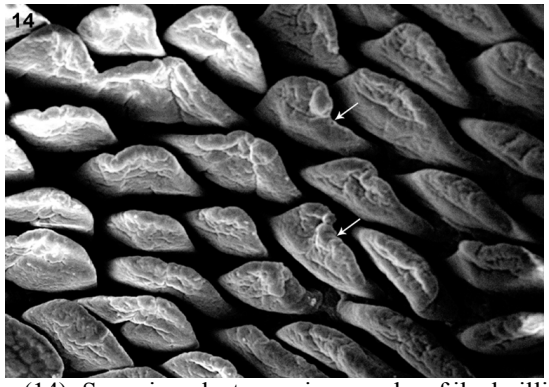

Fig. (14): Scanning electron micrographs of ileal villi of glabridin treated diabetic group showing villi appeared to have normal surface epithelium with goblet cells openings and some villi still show sloughing of their tips (→). (x 100)

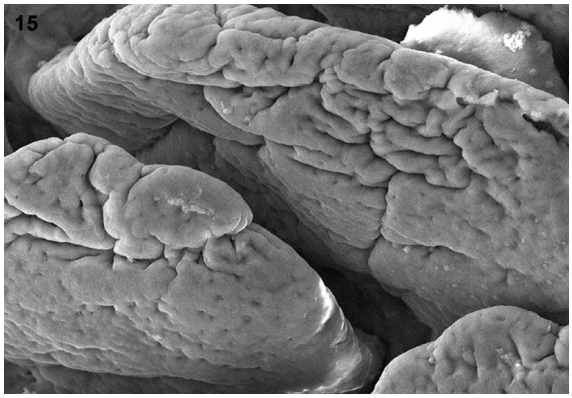

Fig. (15): Scanning electron micrographs of ileal villi of glabridin treated diabetic group showing the villous more or less normal appearance. (x 350)

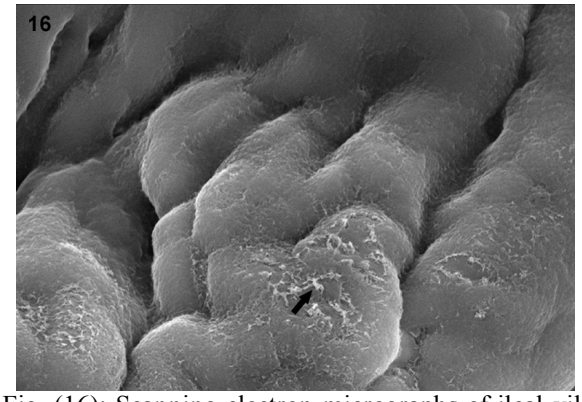

Fig. (16): Scanning electron micrographs of ileal villi of glabridin treated diabetic group showing villous revealed normal surface epithelium and microvilli on the surface appeared nearly normal with mucous secretions of numerous goblet cells (⟨). (x 2000)

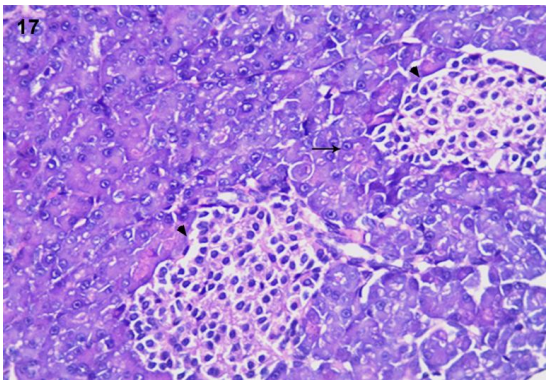

Fig. (17): A photomicrograph of rat pancreas from the control group showing the closely packed pancreatic acini composed of pyramidal shaped cells with rounded pale stained nuclei (→) surrounded by basophilic cytoplasm and apices of the cells are packed with eosinophilic granules, the pale-stained islets of Langerhans (►) scattered inbetween acini. (H & E, Mic. Mag. x 400)

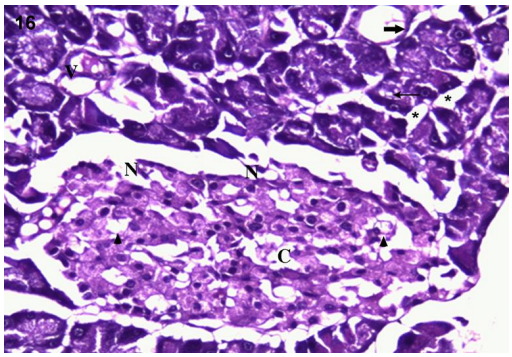

Fig. (18): Photomicrographs of rat pancreas from the diabetic group showing disturbance of the acinar pattern structure, pyknotic nuclei of some acinar cells with severely damaged vacuolated acini (→). Islets with irregular outline, decrease populated cells and homogenization of the center (C), some islet-cells showing pyknotic nuclei (N), ballooning of cells and vacuolated cytoplasm (►). Notice congestion of a blood vessel (V) and detached endothelial lining (⟨) with wide interstitial tissue (*). (H & E, Mic, Mag. x 400)

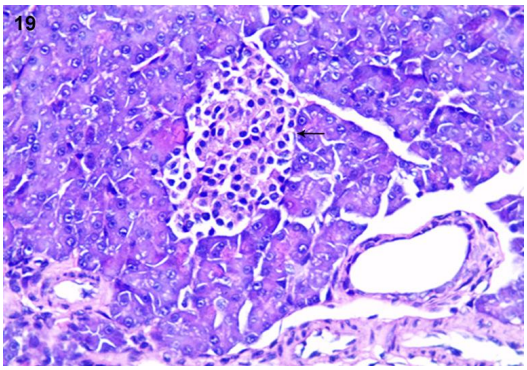

Fig. (19): Photomicrograph of rat pancreas from glabridin treated diabetic group showing nearly normal pancreatic architecture, and an islet with normal appearance (→). (H & E, Mic. Mag. x 400)

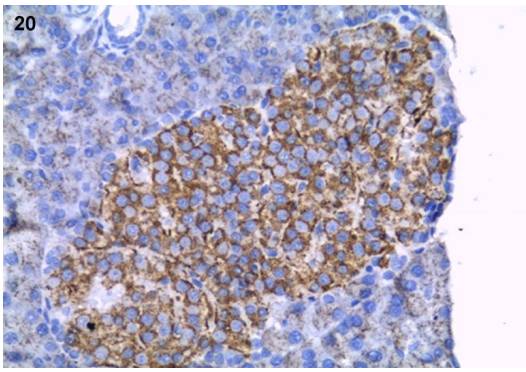

Fig. (20): Photomicrograph of a section in rat pancreas of control group showing positive immunostaining occupying a typical component of β cells in most of the islet cells. (x 400)

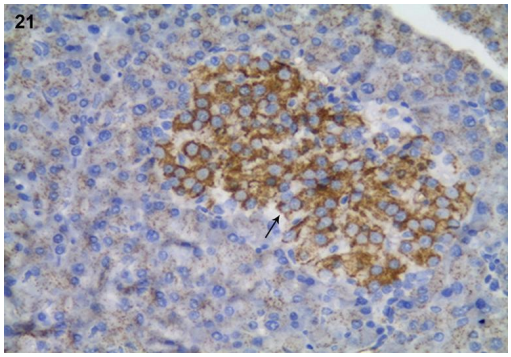

Fig. (21): Photomicrograph of a section in rat pancreas of diabetic group showing few positive stained insulin immunoreactive β cells (→) in pancreatic islet. (x 400)

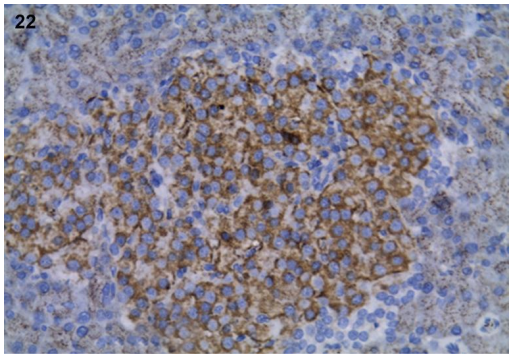

Fig. (22): Photomicrograph of a section in rat pancreas of glabridin treated diabetic group showing a clear increase in the positive immunostaing for insulin of β cells in pancreatic islet. (x 400)

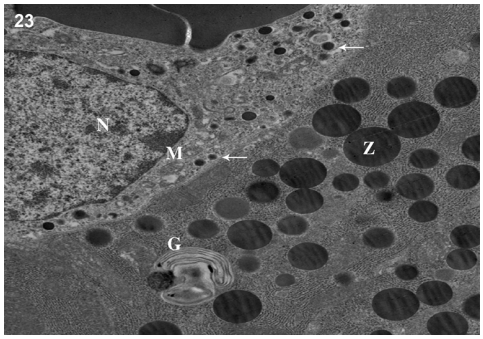

Fig. (23): An electron micrograph of rat pancreas from the control group showing exocrine acinar cells containing zymogen granules (Z), numerous cisternae of RER, well developed Golgi apparatus (G) and endocrine β-cells with dispersed chromatin in its nucleus (N), β granules (→) have dark central core surrounded by an electron lucent halo and mitochondria (M). (Mic. Mag x 2500).

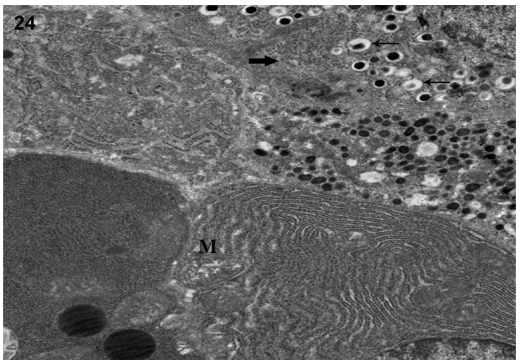

Fig. (24): An electron micrograph of rat pancreas from the diabetic group showing endocrine β-cell of islet with increase in the halo spaces areas around β granules (→) and dilatation of RER (⟨) with damaged and vacuolized mitochondria in the acinar cell (M). (Mic. Mag. x 2500)

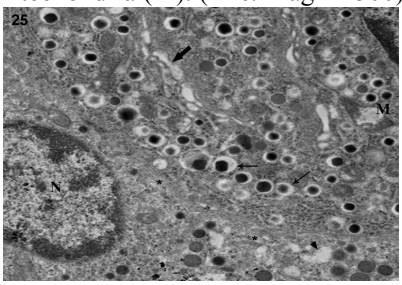

Fig. (25): An electron micrograph of rat pancreas from the diabetic group showing an endocrine β-cell of islet containing vacuolized mitochondria (M) lost their cristae, dilated cisternae of RER (⟨) and increase in the halo spaces areas around β granules (→) with electron lucent vacuoles (►). Notes other β-cell with euchromatin in its nucleus (N) and depletion of β-granules (*). (Mic. Mag. x 4000)

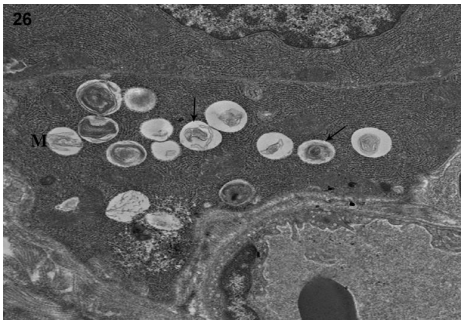

Fig. (26): An electron micrograph of rat pancreas from the diabetic group showing exocrine acinar cell with marked degenerative changes, decrease secretory granules, appearance of autophagic vacuoles (→) and destroyed mitochondria (M). (Mic. Mag. x 3000).

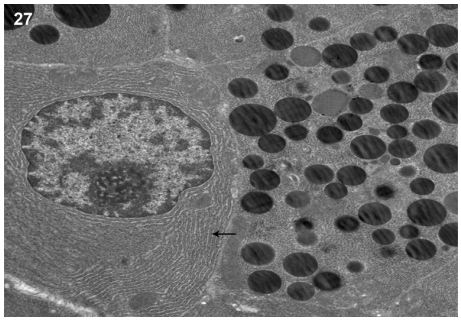

Fig. (27): An electron micrograph of rat pancreas from glabridin treated diabetic group showing exocrine acinar cells with dilatation of RER (→) and increased zymogen granules. (Mic. Mag. x 2000)

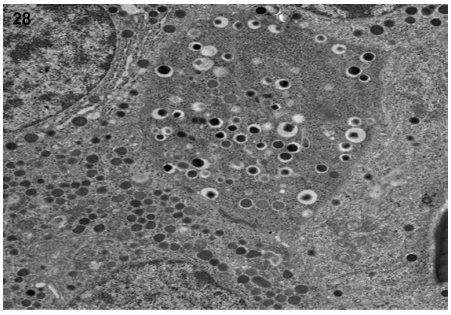

Fig. (28): An electron micrograph of rat pancreas from glabridin treated diabetic group showing endocrine β-cells apparently had retained their morphology and cellular organelles with normal appearance of β-granules. (Mic. Mag. x 2500).

4. Discussion:

Results obtained in the present work showed that many histological changes appeared in ileum of diabetic rats. Ileal villi pleomorphism, cellular infiltration in the corium, sloughing of the columnar cells at the tip of these villi with significant increase in villi height, deep crypts and in muscle layer thickness were observed. In agreement with these results, *Sen, (2011)* contributed mucosal hyperplasia to hyperphagia, overproduction of gastrin, growth hormone and increased level of glucagons-like peptide-2, up-regulation of cell proliferation and inhibition of cell death via apoptosis. In respect to the integrity of gastrointestinal tract lining epithelium, it depends on the balance between the cell proliferation, cell migration and cellular death via apoptosis. Several experimental studies have shown that cell proliferation increases significantly in experimental induced diabetes due to gut trophic hormones or to neuronal loss *(Sen et al., 2011)*. Moreover, sloughing of the surface epithelium and the necrotic cells in some parts of the villi could be interpreted to be due to decreased blood supply as a result of diabetic microangiopathy *(De-Las-Cases and Finely, 1999)*. Cellular infiltration observed in ileal villi of diabetic rats was attributed to bacterial overgrowth and parasitic infestation as reported by previous research work *(Virally-Monod et al., 1998)*. Homogenous material was observed in the core of the villi in diabetic rats. This also was noticed by a previous study, who explained this to be due to edema as a result of diabetic microangiopathy *(De-Las-Casas and Finley 1999)*.

In the present study, scanning electron microscopic examination showed that the ileal villi appeared wide with marked convolutions. This was explained by *Tahara and Yamamoto, (1988)* who reported that disturbance in maturation of the absorptive cells at the villous tips induced abnormal cell kinetics in the ileal cell turnover and would also produced abnormal distinct convolusions of the villous surface in the ileum with diabetes. Also, diabetic microangiopathy explained necrotic areas seen on some villi tips in SEM *(Massimino et al., 1998)*.

The present study showed that diabetes was implicated in pancreatic islets β-cell histomorphological changes. The emerged results indicate severe light and electron micrograph changes in the form of depletion of β-cell granules, severe vacuolation in the islets, pyknotic β-cell nuclei, degenerative and shrunken pancreatic islets of Langerhans, and dissolution of mitochondria. Also there were small diameter, ill defined border of islets of Langerhans with moderate insulin immunoreactivity and decreased number of β-cell per ilset. In coincidence, previous study contributed decreased granules in the cytoplasm usually encountered in insulin dependent diabetes due to the decrease in insulin production or depletion of secretory stores of insulin in damaged cells. Moreover, the observed vacuoles may be due to increased cellular damage. In the present work variable changes in nuclei of islets of diabetic pancreas, some appeared vesicular, others pyknotic nuclei where the euchromatin predominates over the heterochromatin. These changes were in agreement with previous study that suggest this may be due to condensation and shrinkage of the nuclear material *(Arulselvan and Subramanian, 2007)*.

Increase in lipid peroxidation levels, elevation in activities of catalase, superoxide dismutase and decreased activity of glutathion peroxidase were recorded in diabetic rats. These results are indicative of oxidative stress. In this concern, *Baynes, (1991*) reported that hyperglycemia is one of the factors responsible for free radicals generation in diabetes. Also, *Bhor (2004*) mentioned that oxidative damage occurred in small intestine during experimental diabetes. Ultrastructural changes such as mitochondrial vacuolation and dissolution beside dilated RER cisternae were observed in the present work. *Bhor (2004*) documented that lipid peroxides produced by hydroxyl radicals affect mitochondrial function. Free radicals exert their cytotoxic effect by peroxidation of membrane phospholipids leading to increase permeability and loss of membrane integrity *(Kakkar, 1998)*.

Administration of glabridin to diabetic rats improved the histological and the ultrastructural changes together with reduction in the level of lipid peroxidation and increase in the activities of SOD and CAT. Also glabridin was sufficient to reduce triglycerides and cholesterol levels but caused mild glucose level alteration in diabetic treated rats. The mechanisms of glabridin action was attributed to its antioxidant activity *(Ito et al., 2007)*, potential role in stimulating cellular antioxidant defense system against oxidative damage and its estrogenic activity through upregulation expression of mitochondrial antioxidant enzymes *(Haraguchi et al., 2000)*. *Fuharman et al., (2000)* found that the antioxidant effect of glabridin resides mainly in 2 hydroxyl group of the isoflavan ring β. The normalization of hyperlipidemia profiles may contribute in part due to beneficial effects of glabridin on β-cell regeneration and due to protection of LDL by inhibiting the formation of lipid peroxides as reported by previous studies *(Belinky et al., 1998 and Fuharman et al., 2002)*.The increased number of islet cells (including

β-cells) in glabridin treated group may due to its role in β-cell regeneration and antioxidiant properties. This regeneration of the β-cells is probably due to the fact that pancreas contains stable (quiescent) cells which have the capacity of regeneration *(Adeyemi et al., 2010)*.

In conclusion, present results showed that glabridin ameliorated the severity of degenerative changes in STZ-induced diabetes on small intestine and pancreatic β-cells. This effect may be attributed to the antioxidant properties of glabridin.

Corresponding author
Maha M. Abo Gazia
Histology Department, Faculty of Medicine, Al-Fayoum University
mahaabogazia@yahoo.com

References:

Adeyemi, D.O.; Komolafe, O.A.; Adewole, O.S.; Obuotor, E.M.; Abiodun, A.A.; Adenowo, T.K. (2010): Histomorphological and morphometric studies of the pancreatic islet cells of diabetic rats treated with extracts of Annona muricata. Folia Morphologica., 69(2): 92-100.

Aebi, H.E. (1983): Catalase in: Methods of Enzymatic Analysis, 3rd ed., HU Bergmeyer (ed. Verlag Chemie, Weinheim, Flovida, 273-380.

Arulselvan, P.; Subramanian, S. (2007): Beneficial effects of Murraya koenigii leaves on antioxidant defense system and ultrastructural changes of pancreatic cells in experimental diabetes in rats. Chemico-Biological Interactions , 165: 155-164.

Baynes, J.W. (1991): Role of oxidative stress in development of complications in diabetes. Diabetes, 40: 405–412.

Belinky, P.A.; Aviram, M.; Fuhrman, B.; Rosenblat, M.; Vaya, J. (1998): The antioxidative effects of the isoflavan glabridin on endogenous constituents of LDL during its oxidation. Atherosclerosis, 137: 49-61

Bhor, V.M.; Raghuram, N.; Sivakami, S. (2004): Oxidative damage and altered antioxidant enzyme activities in the small intestine of streptozotocin-induced diabetic rats. The International Journal of Biochemistry & Cell Biology ; 36: 89-97.

Chandalia, H.B.; Sadiket, S.; Bhargava, D.K.; Krishnaswamy, P.R. (1980): Estimation of glycosylated haemoglobin by a simple chemical method. Journal of the Association of Physicians of India, 29: 285-286.

Dawson, B.; Trapp, R.G. (2001): Basic and clinical biostatistics. 3rd ed. McGraw-Hill-Appleton and lange: New York, NY.

De-Las-Casas, L.E.; Finley J.L. (1999): Diabetic micro-angiapathy in the small bowel. Histopathology; 35(3): 267-70.

Esterbauer, H.; Cheeseman, K.H. (1990): Determination of aldehydic lipid peroxidation products: Malonaldehyde and 4-hydroxynonenal. Methods in Enzymology, 186; 407-421.

Ettarh, R.R.; Carr K.E. (1997): A morphological study of the enteric mucosal epithelium in the streptozotocin-diabetic mouse. Life Sciences, 61(18): 1851-1858.

Evans, J.L.; Goldfine, I.D.; Maddux, B.A.; Grodsky, G.M. (2003): Are oxidative stress activated signaling pathways mediators of insulin resistance and β-cell dysfunction? Diabetes. 52: 1-8.

Fuhrman, B.; Volkova, N.; Kaplan, M.; Presser, D.; Attias, J.; Hayek, T.; Aviram M. (2002): Antiatherosclerotic effects of licorice extract supplementation on hypercholesterolemic patients: Increased resistance of LDL to atherogenic modifications, reduced plasma lipid levels, and decreased systolic blood pressure. Nutrition, 18: 268-273.

Fukai, T.; Satoh, K.; Nomura, T.; Sakagami, H. (2003): Preliminary evaluation of antinephritis and radical scavenging activities of glabridin from Glycyrrhiza glabra. Fitoterapia; 74:624–9.

Goldstone, L.A. (1983): Under-standing medical statistics. First edition. London William Mairmann. Medical Books Limited.

Haraguchi, H.; Yoshida, N.; Ishikawa, H.; Tamura, Y.; Mizutani, K.; Kinoshita T. (2000): Protection of mitochondrial functions against oxidative stress by isoflavans from Glycyrrhiza glabra. Journal of Pharmacy and Pharmacology, 52: 219-231.

Hayat, M.A. (1981): Fixation for electron microscopy. A Cademic Press.

Hayat, M.A. (1989): Principles and techniques of electrom microscopy: Biological applications. 3rd ed. CRC Press, Inc.: Boca Raton, Florida.

Ito, C.; Oi, N.; Hashimoto, T.; Nakabayashi, H.; Aoki, F.; Tominaga, Y.; Yokota, S.; Hosoe K.; Kanazawa K. (2007): Absorption of dietary licorice isoflavan glabridin to blood circulation in rats. Journal of Nutritional Science and Vitaminology, 53: 358-365.

Kakkar, R.; Kalra, J.; Mantha, S.V.; Prasad K. (1995): Lipid peroxidation and activity of antioxidant enzymes in diabetic rats. Molecular and Cellular Biochemistry; 151: 113-119.

Kakkar, R.; Mantha, S.V.; Radhi, J.; Prasad, K.; Kalra, J. (1998): Increased oxidative stress in rat liver and pancreas during progression of STZ-induced diabetes. Clinical Science, 94: 623-632.

Kiernan, J.A. (2000): Histological and histochemical method: Theory and practice. 3rd ed. Oxford, Boston, Johannesburg, New Delhi.

Kow, Y.Y. (1977): Cell kinetics in the small intestine of suckling rats. I. Influence of hypophysectomy. The Anatomical Record., (188): 69-76.

Marklund, S.; Marklund G. (1974): Involvement of superoxide anion radical in the auto-oxidation of pyrogallol and a convenient assay for superoxide dismutase. European Journal of Biochemistry, 1974; 47: 469-474.

Massimino, S.P.; McBurney, M.I.; Field, C.J.; Thomson, A.B.; Keelan, M.; Hayek, M.G.; Sunvold, G.D. (1998): Fermentable dietary fiber increases GLP-1 secretion and improves glucose homeostasis despite intestinal glucose transport capacity in healthy dogs.

Journal of Nutrition. Oct, 128(10): 1786-93

McGowan, M.W.; Triss, J.D.; Strandbergh, D.R.; Zak B. (1983): A peroxidase-coupled method for the colorimetric determination of serum triglycerides. Clinical Chemistry; 29: 538-542.

Nakagawa, K.; Kishida, H.; Arai, N.; Nishiyam, T., Mae T. (2004): Licorice flavonoids suppress abdominal fat accumulation and increase in blood glucose level in obese diabetic KK-A mice. Biological and Pharmaceutical Bulletin, 27: 1775-1778.

Rotruck, J.T.; Pope, A.L.; Ganther, H.E.; Hafner D.G.; Hoekstra, W.G. (1973): Selenium: Biochemical role as a component of glutathione peroxidase. Science, 179: 588-590.

Rumpler, W.V.; Baer, D.J.; Rhodes D.G. (1998): Energy available from corn oil is not different than that from beef tallow in high or low fiber diets fed to humans. Journal of Nutrition. Dec, 128(12): 2374-82.

Sen, S.; Roy M.; Chakraborti A.S. (2011): Ameliorative effects of glycyrrhizin on streptozotocin-induced diabetes in rats. Journal of Pharmacy and Pharmacology; 63: 287-296.

Tahara, T.; Yamamoto T. (1988): Morphological changes of the villous microvascular architecture and intestinal growth in rats with streptozotocin-induced diabetes. Virchows Archiv. A, Pathological Anatomy and Histopathology, 413:151–158.

Trinder P. (1969): Determination of blood glucose using an oxidase-peroxidase system with a non-carcinogenic chromogen. Journal of Clinical Pathology , 22: 158-161.

Virally-Monod, M.; Tielmans, D.; Kevorkian, J.P.; Bouhnik, Y.; Flourie, B.; Porokhov, B.; Ajzenberg, C.; Warnet A.; Guillausseau P.J. (1998): Chronic diarrhea and diabetes mellitus: prevalence of small intestinal bacterial overgrowth. Diabetes & Metabolism Dec, 24(6): 530-6.

Wybenga, D.R.; Pileggi V.J.; Dirstine, H.; Giorgio J.D. (1970): Direct manual determination of serum total cholesterol with a single stable agent. Clinical Chemistry; 16: 980-984.

Zoubi, S.A.; Mayhew, T.M.; Sparrow, R.A. (1995): The small intestine in experimental diabetes: Cellular adaptation in crypts and villi at different longitudinal sites. Virchows Archiv; 426:501-507.

2/25/12